ELSEVIER
Theoretical and Applied Fracture Mechanics 38 (2002) 165–175
theoretical and applied fracture mechanics
www.elsevier.com/locate/tafmec

Energy release rates in a constrained epoxy disc with Hookean and Mooney–Rivlin materials

R.C. Batra *, H.K. Ching

Department of Engineering Science and Mechanics, Virginia Polytechnic Institute and State University, MC 0219, Blacksburg, VA 24061, USA

Abstract

Assuming that the disc material can be modeled either as Mooney–Rivlin or as Hookean and the steel ring enclosing the disc as Hookean, the energy release rates as a function of the crack length are evaluated and compared. Two loadings are considered—one in which the surface of the star shape hole in the disc is loaded by a uniform pressure and the other in which the temperature of the composite body is uniformly raised. It is found that the linear and the nonlinear analyses give qualitatively similar results for the two loadings. For each load, the energy release rate increases with an increase in the starter crack length, reaches a maximum value and then decreases gradually.

Keywords: Energy release rate; Mechanical and thermal loads; Finite element solution; Linear and nonlinear analyses

1. Introduction

A common problem in industry is to design a part based on the test data for a simple loading condition such as an uniaxial tension test or a torsion test. Whereas test data from a tension test suffices to determine uniquely the two material parameters for an isotropic linear elastic material, it is usually insufficient for the determination of the constitutive relation for a nonlinear elastic material. Here such a problem for an epoxy is analyzed. Assuming that the epoxy can be modeled as a Mooney–Rivlin material, values of the two material parameters from the uniaxial tension test data are found, and then used to compute the energy release rate as a function of the starter crack length in a circular polymeric disc enclosed in a thin steel ring and having a star shaped hole with six symmetrical leaflets at its center. Two loadings, namely, a uniform pressure on the surface of the hole and a uniform temperature rise of the composite body are considered. The steel ring is modeled as a Hookean material. Computed results are compared with those obtained by modeling the epoxy as a Hookean material. It is found that for both loadings and for each one of the 12 crack lengths considered, the analysis of the nonlinear problem gives a smaller value of the energy release rate than that for the linear problem. Results for the Hookean material vary significantly with values of Poisson's ratio in the range 0.49–0.4999.

* Corresponding author. Tel.: +1-540-231-6051; fax: +1-540-231-4574.

E-mail address: rbatra@vt.edu (R.C. Batra).

PII: S0167-8442(02)00085-X

Since a structure has numerous cracks of varying lengths, this type of analysis will help estimate its useful life.

Many investigations [1–6] on crack tip fields have considered linear strain–displacement relations but nonlinear stress–strain ones. The emphasis has been to derive a path independent integral whose value is a measure of deformation near a crack tip. The often used J-integral was given in [2] and it was stated that this is a special case of the energy momentum tensor introduced in [1]. The energy momentum tensor characterizes generalized forces of dislocations in an elastic field. It is shown in [7] that the energy momentum tensor appropriate for finding the force on a disclination in a nematic liquid crystal is, to within an unimportant hydrostatic pressure, the same as the Ericksen stress tensor [8]. This implies that the so-called configurational force on a disclination in a nematic liquid crystal is in fact a real force exerted on the core of the disclination by the surrounding medium; a similar result is proved in [9] for a nonlinear hyperelastic material. For a straight crack propagating at a uniform speed in a linear or a nonlinear elastic material, a path independent integral was derived in [4] from the balance of total energy which for a mechanical problem is also the first law of thermodynamics. It was shown that this path independent integral equals the energy release rate. Whereas the work employed a nonlinear stress–strain relation, strains were linearly related to displacement gradients. It should be mentioned that path independent integrals were used by Gunter in 1934 although not in the same context.

The work reported in [10] seems to be the first to analyze the problem within the framework of nonlinear elasticity for a neo-Hookean material. The problem of a crack in an infinite, thin and incompressible sheet subjected to biaxial tension at infinity was studied by the method of successive approximations which required that deformations be large throughout the entire sheet. An asymptotic plane strain analysis [11,12] of a symmetrically loaded traction free crack in a slab of compressible hyperelastic material showed that the singular field near the crack tip depends strongly on the behavior of the stored energy at large strains. It has been shown [13] that for a generalized Mooney–Rivlin material, the crack opens up in the neighborhood of its tip even if the applied load is antisymmetric with respect to the crack plane. The nonexistence of an antisymmetric mode due to the nonlinearity of the global crack problems is also exhibited in [13]. An asymptotic analysis of the plane deformation crack problem for compressible rubberlike materials with Ogden–Ball stored energy function that satisfies the polyconvexity and certain growth conditions was performed in [14]. It showed that the degree of singularity and the leading terms of the local deformation field were exactly the same as those obtained in [11,12] even though the constitutive relations in the two studies were different. For the Ogden–Ball materials the opening angle between the crack faces becomes 180° at the crack tip. The coefficient of the canonical field, which is called the stress intensity factor, can be found only after the global crack problem has been solved.

Mode-I and mixed mode deformations of a crack in a homogeneous sheet made of a generalized neo-Hookean material, analyzed in [15], showed that there exists more than one singular term and the leading singularity is stronger than that predicted by the linearized theory. Whereas these studies considered traction free crack surfaces, the effect of nonconservative surface tractions applied to the crack faces on the energy release rate for two-dimensional problems was scrutinized in [16]. This work discussed the modification to be made in the usual expression for the energy release rate and also demonstrated that the energy release rate depends upon the constitutive relation used to model the material response. For the problem studied here, numerical solutions indicate that the orders of singularity for the linear and the nonlinear analyses are the same. At a point near the crack tip, the normal strains predicted by the two analyses are nearly the same but the shear strains are different.

2. Formulation of the problem

Fig. 1 shows a cross-section of the composite cylindrical body whose length is very large as compared to its diameter. Thus a plane strain state

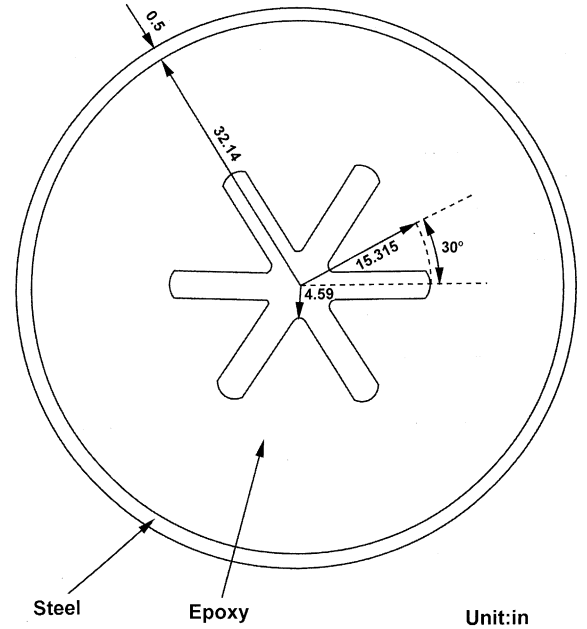

Fig. 1. A cross-section of the composite cylindrical body whose plane strain deformations are studied.

of deformation is assumed to prevail in the body. The star shaped hole at the center has six symmetrically located leaflets; dimensions of different parts are shown in Fig. 1. The epoxy and the steel casing are modeled as isotropic and homogeneous materials. Initially the body is stress free and at a uniform temperature. Deformations of the body under two types of loads, namely, a uniform pressure on the inner surface of the hole and a uniform temperature rise of the entire body are studied. In each case, the outer surface of the steel ring is taken to be traction free. Because of the symmetry of the geometry and the loading conditions, deformations of only a 30° sector of the body are investigated. Points on the bounding surfaces $\theta = 0°$ and $\theta = 30°$ are constrained to move radially, and tangential tractions on these surfaces are set equal to zero. The epoxy disc is assumed to be perfectly bonded to the steel ring so that displacements and surface tractions are continuous across their common interface.

The referential description of motion is employed to describe deformations of the body, and analyze the static problem. Displacements of a material point are found from the balance of linear momentum and the moment of momentum subject to the aforestated boundary conditions and the following constitutive relations. Deformations of the steel ring are assumed to be infinitesimal and its isotropic material modeled by Hooke's law with Young's modulus = 29 Mpsi, Poisson's ratio = 0.3, and the coefficient of thermal expansion = 6.5×10^{-6}/°F.

The epoxy is modeled either as a Mooney–Rivlin material or as a Hookean material. For the Mooney–Rivlin material

$$W = C_{10}(\bar{I}_1 - 3) + C_{01}(\bar{I}_2 - 3) + \frac{1}{D_1}(J^{\mathrm{el}} - 1)^2, \quad (1)$$

where W is the strain energy per unit volume in the reference configuration; C_{10}, C_{01}, and D_1 are temperature dependent material parameters; $\bar{I}_1$ and $\bar{I}_2$ are the first and the second invariants of the deviatoric strain tensor, and are defined as

$$\bar{I}_1 = \bar{\lambda}_1^2 + \bar{\lambda}_2^2 + \bar{\lambda}_3^2, \quad \bar{I}_2 = 1/\bar{\lambda}_1^2 + 1/\bar{\lambda}_2^2 + 1/\bar{\lambda}_3^2. \quad (2)$$

Here $\bar{\lambda}_i = J^{-1/3}\lambda_i$; J equals the determinant of the deformation gradient and λ_1, λ_2, and λ_3 are principal stretches. The shear modulus μ_0 and the bulk modulus K_0 at zero strain are given by

$$\mu_0 = 2(C_{10} + C_{01}), \quad K_0 = 2/D_1. \quad (3)$$

The elastic volume ratio, J^{el}, is related to J by

$$J^{\mathrm{el}} = J/(1 + \alpha\Delta T)^3, \quad (4)$$

where α is the coefficient of thermal expansion and ΔT the change in temperature. For purely mechanical deformations, $\Delta T = 0$, $J^{\mathrm{el}} = J$, and D_1 is assigned a very large value as compared to C_{10} and C_{01} so that deformations are essentially isochoric.

Values of the two material parameters in the Mooney–Rivlin relation found from the uniaxial test data by using the finite element code ABAQUS are

$$C_{10} = 1550 \text{ psi}, \quad C_{01} = -811.1 \text{ psi}. \quad (5)$$

ABAQUS determines material constants through a least-squares-fit procedure which minimizes the relative error in the nominal stress. For n nominal axial stress vs. nominal axial strain data pairs, the error

$$E_{\mathrm{r}} = \sum_{i=1}^{n}(1 - T_i^{\mathrm{com}}/T_i^{\mathrm{test}})^2 \quad (6)$$

is minimized. Here T_i^{test} is a stress value from the test data, and T_i^{com} is the corresponding computed value. Computed values of the axial component of the first Piola–Kirchhoff stress tensor vs. the nominal axial strain which equals the change in length/length are compared with the experimental data in Fig. 2. It is clear that the two sets of data are very close to each other implying thereby that values given in (5) of C_{10} and C_{01} are very good. Comparisons of computed results with test data for different loading configurations are needed to ensure that the Mooney–Rivlin relation models well the epoxy material with values (5) of C_{10} and C_{01}.

In order to delineate effects of material and geometric nonlinearities, the epoxy was also modeled as Hookean with Poisson's ratio varying from 0.49 to 0.4999 and the shear modulus equal to 1477.8 psi. As Poisson's ratio approaches 0.5, the material becomes essentially incompressible and is incompressible for Poisson's ratio equal to 0.5. As shown below, the energy release rate strongly depends upon Poisson's ratio for the Hookean material. The axial stress vs. the axial strain curve for the Hookean material is also depicted in Fig. 2. For both linear and nonlinear analyses, the coefficient of thermal expansion for the epoxy material equaled 5.6×10^{-5}/°F which is a little less than nine times that for the steel.

With the goal of ascertaining the failure characteristics of the epoxy, the energy release rate as a function of the initial crack length was determined. When the inner surface of the hole and the surface of the starter crack aligned with the x_1-axis are loaded by a uniform pressure q, the energy release rate G, for a linear elastic material is given by

$$G = \int_{\Gamma} \left(W n_1 - T_{ij} n_j \frac{\partial u_i}{\partial x_1} \, \mathrm{d}s \right) + \int_{\Gamma_c} q \frac{\partial u_2}{\partial x_1} \, \mathrm{d}x_1, \qquad (7)$$

where W is the strain energy density, $\mathbf{u}$ the displacement of a point, Γ a closed curve enclosing the crack tip, $\mathbf{n}$ the outward unit normal to Γ, T_{ij} the stress tensor, a repeated index implies summation over the range of the index, and Γ_c the two crack faces. Note that the last term on the right-hand side of (7) represents the work done by the pressure on the crack surfaces. For the thermal load, there is no surface traction on the crack surface and this term makes no contribution to the value of G. For a homogeneous hyperelastic material, T_{ij} equals the first Piola–Kirchhoff stress tensor.

For the linear elastic problem, the value of the energy release rate will vary approximately as the reciprocal of Young's modulus for the epoxy because the epoxy disc is enclosed in a steel ring which will apply different tractions on the outer surface of the epoxy disc when its Young's modulus is varied. Numerical experiments indicated that $G \propto 1/E$ is valid for the present problem since the steel ring is located far from the crack tip. However, no such conclusion can be drawn for the Mooney–Rivlin material. Furthermore, for the Hookean material, $G \propto q^2$, and this proportionality relation is not valid for the Mooney–Rivlin material. Values of material parameters for five nonlinear materials from the same tension test data were found in [16] and the variation of the computed value of the energy release rate with the pressure q on the crack faces was found to be different for these materials.

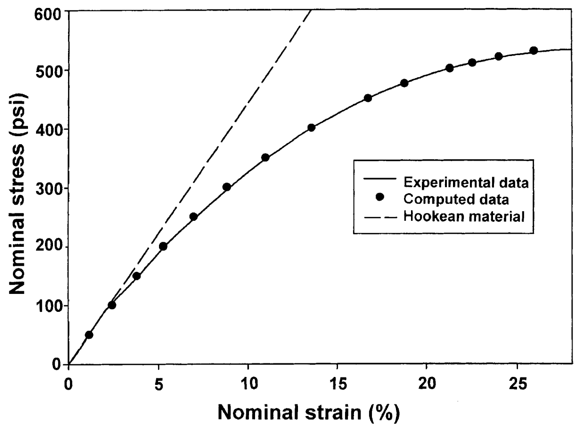

Fig. 2. A comparison of the computed and the experimental axial nominal stress—axial engineering strain curves for the disk material.

3. Computation and discussion of results

Because of the complicated geometry and the nonlinearities considered, the problem was analyzed by the finite element method with the commercial code ABAQUS 6.11. The region in the 30°

sector was divided into 4824 CPE8H (8-node element with biquadratic interpolation for displacements and linear interpolation for the pressure field) quadrilateral elements with smaller elements near the crack tip. Since the order of singularity at the crack tip for the Mooney–Rivlin material is not well established, the node on a side of an actual element was located at the midpoint of the side. As shown in Fig. 3, the element size increased gradually with the distance from the crack tip. Two different finite element meshes—one with 2412 elements and the other with 4824 elements—were used to decipher the effect of discretization of the domain on the computed results. No appreciable difference between the two sets of results was found; results reported herein are with the mesh of 4824 elements. For a starter crack of length 1 in., Fig. 4 exhibits the finite element mesh

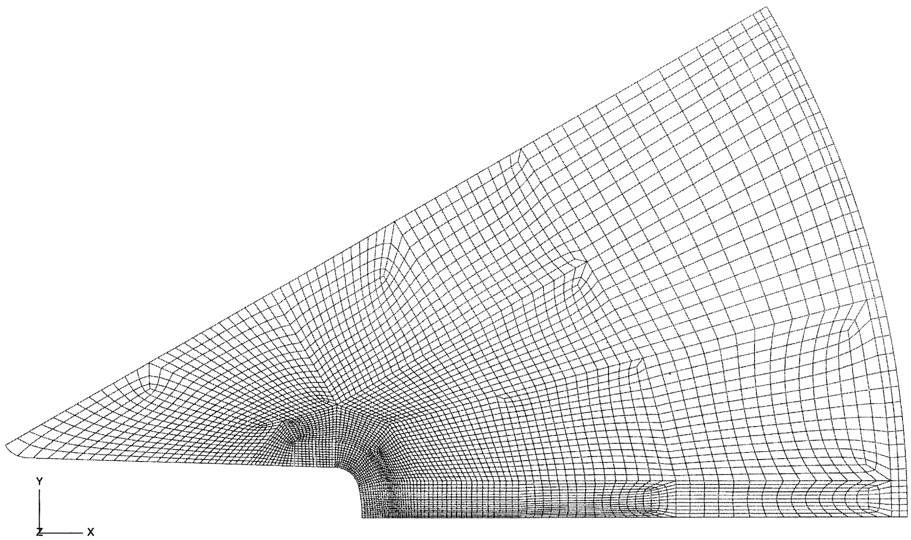

Fig. 3. A finite element mesh with 4824 elements used for the analysis of the problem.

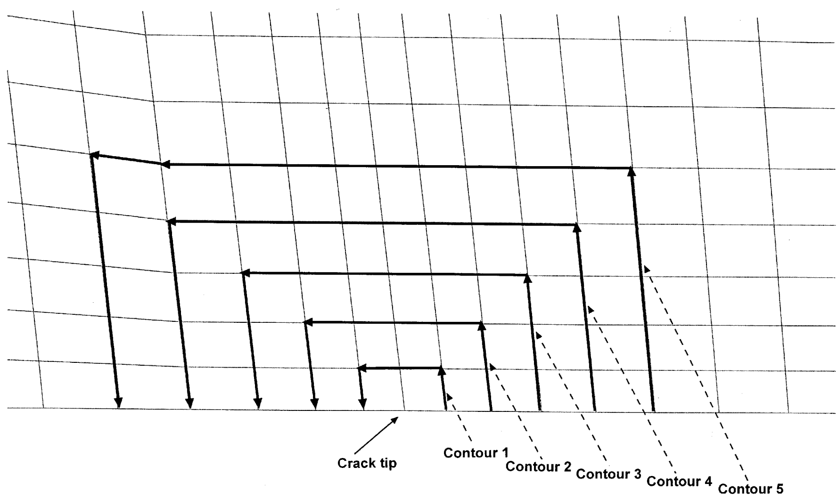

Fig. 4. Finite element mesh around the crack tip, and five contours used to compute the energy release rate.

around the crack tip and five contours used to compute the energy release rate. These contours are comprised of boundaries of consecutive elements in the neighborhood of the crack tip; the first contour starts from the edge of the first element with one node at the crack tip, the second one from the edge of the second element, etc. Distances from the crack tip along the positive x_1-axis of these five contours equal 0.039, 0.081, 0.127, 0.178 and 0.232 in. respectively.

3.1. Effect of Poisson's ratio

For 1000 psi pressure applied on the surface of the hole and faces of 1-in. long crack, Fig. 5 depicts the dependence of the energy release rate upon Poisson's ratio, ν, of the disc modeled as a Hookean material. It is clear that the value of the energy release rate depends strongly upon ν. A close examination of the computed stresses and strains indicated that the hydrostatic pressure,

$$p = \frac{2\mu_0 \nu}{(1-2\nu)} \varepsilon_{ii} \tag{8}$$

varied noticeably when ν was increased from 0.49 to 0.4999. In Eq. (8) ε_{ij} is the infinitesimal strain tensor. An increase in ν decreases the compressibility of the material which reduces significantly the opening between the crack faces created by the

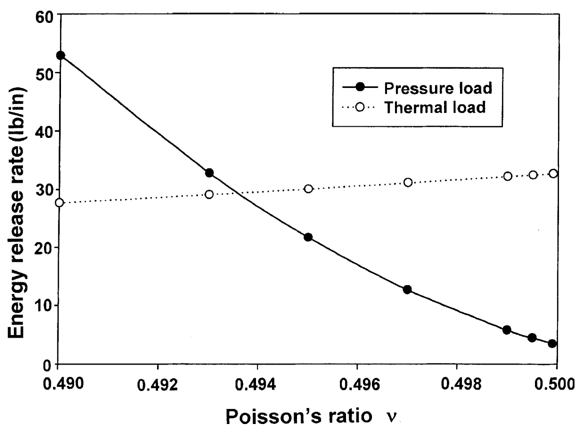

Fig. 5. For 1000 psi pressure and initial crack length of 1 in., dependence of the value of the energy release rate upon Poisson's ratio, ν. The dependence of the energy release rate upon ν is also shown for a thermal load of 85 °F.

pressure acting on them. This is evident from the deformed shapes of the crack face plotted in Fig. 6a for different values of ν; note that the vertical scale is much expanded. Vertical displacements in the direction of the applied pressure of points on the crack faces decrease with an increase in Poisson's ratio. The curvature of the deformed crack tip increases with an increase in Poisson's ratio. Higher values of the vertical displacement of points on the crack face result in larger values of the work done by the pressure q acting on the crack face and increase noticeably the contribution to the energy release rate made by the last term on the right-hand side of Eq. (7).

For a temperature increase of 85 °F, values of the energy release rate, plotted in Fig. 5, do not vary much when ν is increased from 0.490 to 0.4999 mainly because the last term on the right-hand side of Eq. (7) makes null contribution to the energy release rate.

Fig. 6b evinces the variation of the infinitesimal shear strain $\varepsilon_{xy} = \varepsilon_{12}$ at points near the crack tip and lying on the axis of the crack; the abcissa r equals the distance of a point from the crack tip. It is clear that Poisson's ratio significantly influences the distribution of the shear strain at points in the vicinity of the crack tip and the order of singularity increases with a decrease in Poisson's ratio from 0.4999 to 0.49.

Variations of the values of the the energy release rate with the length of the starter crack for Poisson's ratio = 0.49, 0.495, 0.499 and 0.4999 are depicted in Fig. 6c. Results are qualitatively similar in that for every length of the starter crack, the value of the energy release rate diminishes with an increase in Poisson's ratio.

Recalling that the Mooney–Rivlin material is incompressible, ν is henceforth set equal to 0.4999 for the Hookean material in comparing results of linear and nonlinear analyses.

3.2. Pressure load

For an internal pressure of 1000 psi, Table 1 lists values of the energy release rate for different starter crack lengths and the five contours. Except for the case of the very short starter crack of length 0.05 in., the five values of the energy release rate

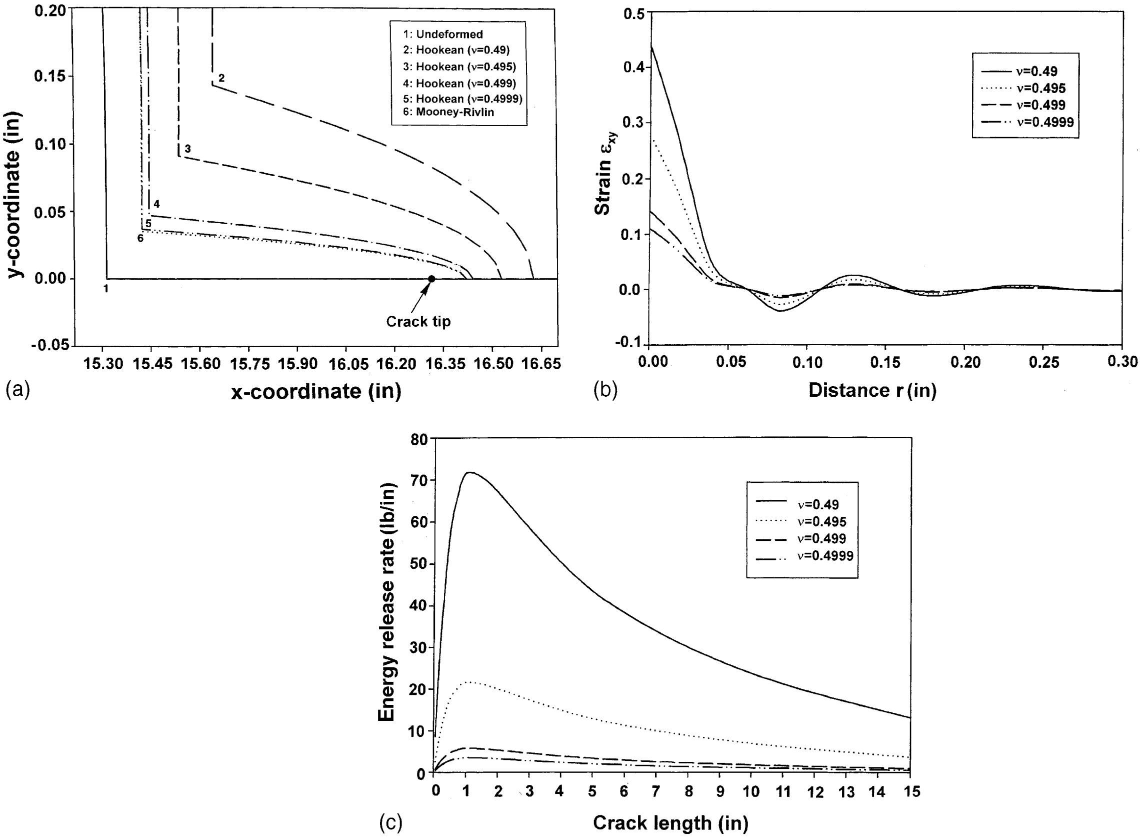

Fig. 6. (a) Deformed shapes of the crack face for different values of Poisson's ratio. (b) For Poisson's ratio equal to 0.49, 0.495, 0.499 and 0.4999 variation with the distance from the crack tip of the infinitesimal shear strain ε_{xy}. (c) For a pressure of 1000 psi, variation of the energy release rate with the length of the starter crack for four values of Poisson's ratio.

are within 2.5% of each other implying that the integral is path independent. Fig. 7 evinces for the linear and the nonlinear analyses the dependence of the energy release rate on the length of the starter crack. In each case the energy release rate initially increases with an increase in the crack length, reaches a maximum value at a crack length of about 1.0 in. for the linear analysis and about 0.8 in. for the nonlinear analysis and then gradually decreases with an increase in the crack length. The two analyses give qualitatively similar results and the linear analysis gives ≈20% higher value of the the energy release rate. Note that in the nonlinear problem, the tangent modulus decreases with an increase in the strain at a point and thus the material exhibits softening behavior. Recall that in the linear problem, $G \propto 1/E$, intuitively one will expect that G for the nonlinear problem should be higher than that for the linear problem. However, such is not the case. Contributions for the two cases to the energy release rate made by the last term on the right-hand side of Eq. (7) are the same since as shown in Fig. 6a the deformed shapes of the crack face coincide with each other. The difference in the values of the energy release rate in the two cases must come from the first term on the right-hand side of Eq. (7). In an attempt to delineate the order of singularity at the crack tip, for a 1-in. starter crack the variation with the distance from the crack tip of the components $\varepsilon_{xx}(E_{xx})$, $\varepsilon_{yy}(E_{yy})$ and $\varepsilon_{xy}(E_{xy})$ of the strain at points on the x_1-axis is plotted in Fig. 8. Here E_{ij} are components of the Green–St. Venant strain tensor and differ from those of ε_{ij} in quadratic terms in

Table 1
Values of the energy release rate computed with the five contours for an internal pressure of 1000 psi, and different starter crack lengths

Starter crack's length (in.)	Analysis type	Contour				
		1	2	3	4	5
0.05	Linear	0.4166	0.4277	0.4266	0.4268	0.5479
	Nonlinear	0.3563	0.3581	0.3606	0.3640	0.4099
0.1	Linear	0.8143	0.8262	0.8232	0.8234	0.8232
	Nonlinear	0.6883	0.6788	0.6816	0.6897	0.6911
0.2	Linear	1.498	1.525	1.518	1.518	1.518
	Nonlinear	1.209	1.166	1.163	1.175	1.182
0.4	Linear	2.490	2.529	2.518	2.519	2.519
	Nonlinear	2.086	2.026	2.021	2.045	2.055
0.6	Linear	3.006	3.115	3.113	3.114	3.114
	Nonlinear	2.415	2.354	2.350	2.371	2.381
0.8	Linear	3.360	3.429	3.418	3.420	3.420
	Nonlinear	2.761	2.640	2.616	2.636	2.642
1.0	Linear	3.423	3.549	3.546	3.546	3.547
	Nonlinear	2.724	2.609	2.584	2.596	2.602
2.0	Linear	3.211	3.276	3.264	3.265	3.264
	Nonlinear	2.704	2.593	2.560	2.569	2.568
4.0	Linear	2.354	2.384	2.374	2.375	2.375
	Nonlinear	2.148	2.126	2.119	2.136	2.143
5.0	Linear	1.996	2.054	2.045	2.045	2.045
	Nonlinear	1.731	1.704	1.689	1.696	1.697
10.0	Linear	1.063	1.091	1.086	1.086	1.086
	Nonlinear	0.9492	0.9506	0.9458	0.9500	0.9513
15.0	Linear	0.5633	0.5801	0.5774	0.5774	0.5774
	Nonlinear	0.5363	0.5387	0.5334	0.5332	0.5321

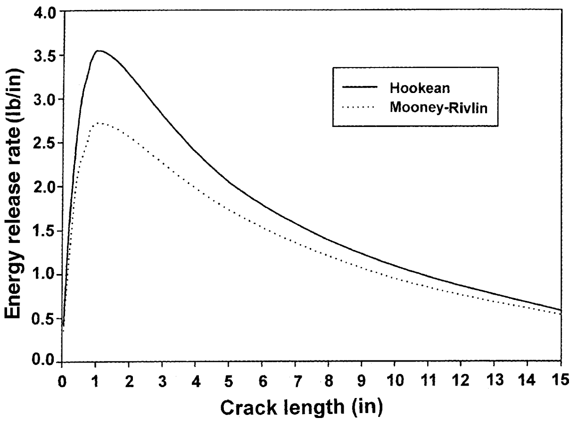

Fig. 7. Variation of the energy release rate with the crack length when the disk material is modeled either as a Hookean material or as a Mooney–Rivlin material.

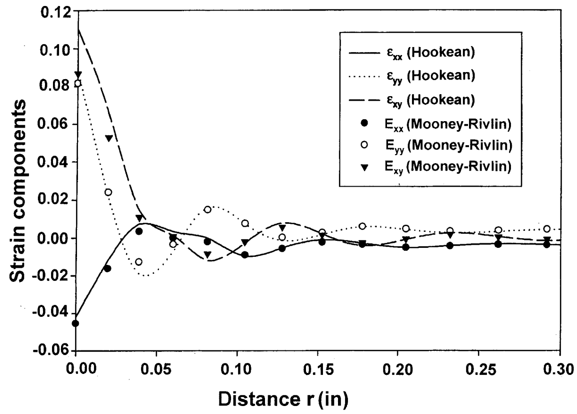

Fig. 8. For the linear and the nonlinear analyses, variation with the distance from the crack tip of strain components at points directly ahead of the starter crack of length 1 in.

the displacement gradients. It is clear that the magnitude of each strain component at the crack tip for the linear analysis is a little higher than that for the nonlinear analysis. However, at points on the x_1-axis whose distance ahead of the crack tip is more than 10% of the starter crack length, the two analyses give nearly the same values of strains. As exhibited in Fig. 6a, the crack tip is blunted for the two analyses. For a starter crack of length 1 in., the maximum in-plane principal stress induced at a point near the crack tip is compressive and its magnitude equals 219.96 and 261.06 psi respectively for the linear and the nonlinear analyses; the corresponding values of the maximum in-plane principal strains are 0.1231 and 0.1229. It is clear that the limit of validity of infinitesimal deformations has been exceeded.

Fig. 9 exhibits contours of the maximum principal strain in a small region around the crack tip for the two analyses. In each case, only a small region around the crack tip is intensely deformed, and contours of the principal strain look alike. Contour plots of the maximum in-plane principal stress for the two analyses are also very similar to each other and are therefore omitted.

For a starter crack of length 1 in., the variation of the value of the energy release rate with the pressure q applied on the surfaces of the hole and the crack is plotted in Fig. 10. One can verify that for the Hookean material the value of the energy release rate is proportional to q^2. Plots of Fig. 10 reveal that the value of the energy release rate for the Mooney–Rivlin material is smaller than that for the Hookean material and the difference between the two increases with an increase in the applied pressure q.

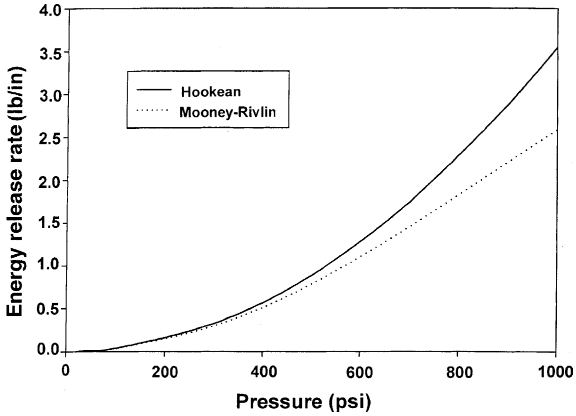

Fig. 10. For a crack of length 1 in., variation of the value of the energy release rate with the applied pressure q for the linear and the nonlinear analyses.

3.3. Thermal load

The temperature of the disk and the steel ring was increased by 85° F, and the coefficients of thermal expansion for the epoxy and the steel were set equal to 5.6×10^{-5}/°F and 6.5×10^{-6}/°F respectively. For both linear and nonlinear analyses, values of the energy release rate for each one of the five contours depicted in Fig. 4 were found to be essentially the same. Fig. 11 shows the variation of

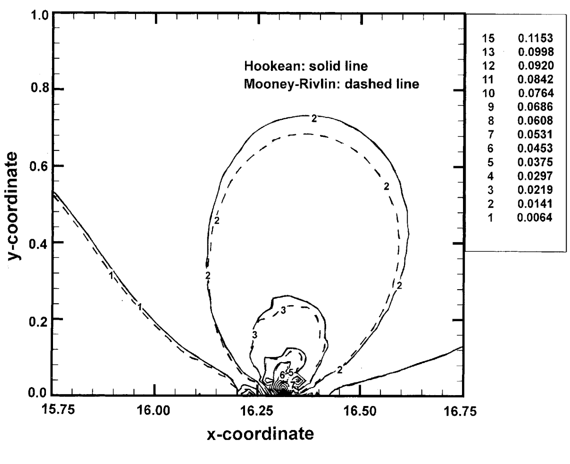

Fig. 9. Contours of the in-plane maximum principal strain in a small region around the crack tip of 1 in. long crack and applied pressure of 1000 psi.

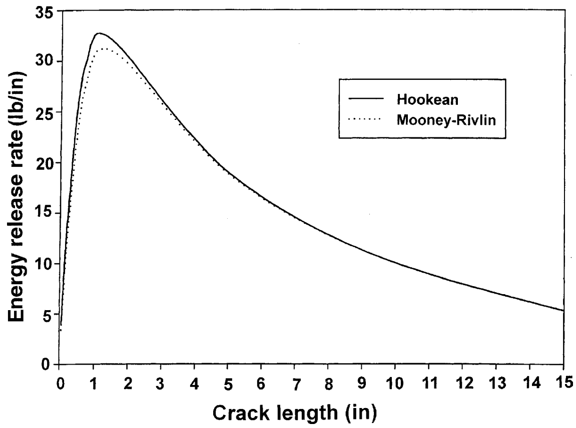

Fig. 11. Variation of the energy release rate with the crack length for the thermal loading.

the energy release rate with the crack length for the two analyses. The two sets of results agree qualitatively and quantitatively also. For the two analyses the maximum value of the energy release rate occurs for a crack of length 1 in. after which it gradually decreases with an increase in the crack length. As for the thermal loading, the energy release rate for the nonlinear analysis is smaller than that for the linear analysis but the difference between the two is perceptible only when the length of the starter crack is less than 4 in. For the two analyses, the variation of the energy release rate with the temperature rise is parabolic. For a starter crack of length 1 in. and 85 ° F temperature rise, the variation with the distance from the crack tip of different components of strain at points ahead of the crack tip and located on the x_1-axis is plotted in Fig. 12. Whereas for the linear problem, all components of the in-plane strain tensor exhibit a singular behavior near the crack tip, for the nonlinear analysis E_{xy} and E_{yy} appear to be singular but E_{xy} is not. As for the pressure loading, large values of strain are confined to points whose distance from the crack tip is <10% of the length of the starter crack. The maximum value of ε_{xy} is nearly 3.5 times that of E_{xy}. However, at a point near the crack tip the magnitude of E_{xx} is about 1.5 times that of ε_{xx} and values of E_{yy} and ε_{yy} are the same. For a crack of length 1 in., the maximum in-plane principal stresses in the epoxy for the linear and the nonlinear analyses equal 2369 and 2276 psi respectively, and the corresponding values of the maximum in-plane principal strains are 0.367 and 0.4156. It is clear that the range of validity of the linear theory has been exceeded.

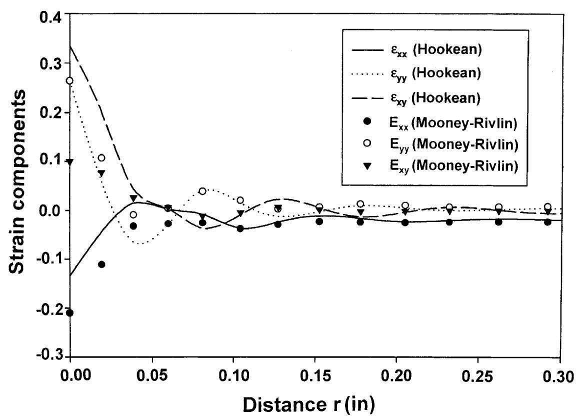

Fig. 12. For the linear and the nonlinear analyses, variation with the distance from the crack tip of strain components at points on the surface of the starter crack of length 1 in. and for a uniform temperature rise of 85 °F.

4. Conclusions

The variation of the energy release rate with the crack length for an epoxy disk with a star shape hole at its center and enclosed in a thin circular steel ring has been studied. Two loadings, namely an internal pressure of 1000 psi and a temperature increase of 85 °F, are considered. The epoxy is modeled either as a Mooney–Rivlin material or as a Hookean material. The value of the energy release rate for a Hookean material strongly depends upon the value assigned to Poisson's ratio, ν. It is found that for $\nu = 0.4999$ the variation of computed values of the energy release rate with the crack length obtained from the linear and the nonlinear analyses agree qualitatively; the value from the linear analysis is about 20% higher than that from the nonlinear analysis. Thus the design based on the linear analysis is conservative. The maximum value of the energy release rate for the linear analysis occurs for a crack of length 1.0 in. but for a crack length of 0.8 in. for the nonlinear analysis. For the thermal load, the two analyses give about the same value of the energy release rate and the maximum value of the energy release rate occurs for a crack length of nearly 1 in.

Even for the linear analysis, values of the energy release rate for the combined thermomechanical load cannot be obtained by adding the energy release rates for the corresponding mechanical and thermal loads since the energy release rate is proportional to the square of the applied pressure and to the square of the temperature change.

It is important that the epoxy be characterized more carefully with the test data from different types of experiments. For the present problem, the linear analysis gives qualitatively correct information and provides a reasonably accurate value of the critical crack length for which the energy release rate is maximum. However, this is not true in general since for the simple shearing problem the linear analysis fails to predict the Poynting effect whereas the nonlinear analysis with a Mooney–Rivlin constitutive relation predicts it. Also, results for the nonlinear analysis will depend upon the constitutive relation used to model the material response since it strongly influences the deformation fields near the crack tip.

References

[1] J.D. Eshelby, The determination of the elastic field of an ellipsoidal inclusion and related problems, Proc. Roy. Soc. London, Ser. A 241 (1957) 376–396.

[2] J.W. Hutchinson, Singular behavior at the end of a tensile crack in a hardening material, J. Mech. Phys. Solids 6 (1968) 13–31.

[3] J.R. Rice, G.F. Rosengren, Plane strain deformation near a crack tip in a power law hardening material, J. Mech. Phys. Solids 16 (1968) 1–12.

[4] G.C. Sih, Dynamic aspects of crack propagation, in: M.F. Kanninen, W.F. Adler, A.P. Rosenfield, R.I. Jaffee (Eds.), Inelastic Behavior of Solids, McGraw-Hill, New York, 1970, pp. 607–639.

[5] C.F. Shih, Small-scale yielding analysis of mixed-mode plane strain crack problems, in: Fracture Analysis ASTM, vol. 560, 1974, pp. 187–210.

[6] S.M. Sharma, N. Aravas, Determination of higher-order terms in asymptotic elastoplastic crack tip solutions, J. Mech. Phys. Solids 39 (8) (1991) 1043–1072.

[7] J.D. Eshelby, The force on a disclination in a liquid crystal, Philos. Mag. 42A (1980) 359–367.

[8] J.L. Ericksen, Equilibrium theory of liquid crystals, in: G. Brown (Ed.), Advances in Liquid Crystals, vol. 2, Academic Press, New York, 1976, pp. 233–298.

[9] R.C. Batra, The force on a lattice defect in an elastic body, J. Elasticity 17 (1987) 3–8.

[10] F.S. Wong, R.T. Shield, Large plane deformations of thin elastic sheets of neo-Hookean material, Z. Angew. Math. Phys. 20 (1969) 176–199.

[11] J.K. Knowles, E. Sternberg, An asymptotic finite-deformation analysis of the elastostatic field near the tip of a crack, J. Elasticity 3 (1973) 67–107.

[12] J.K. Knowles, E. Sternberg, Finite-deformation analysis of the elastostatic field near the tip of a crack: reconsideration and higher order results, J. Elasticity 4 (1974) 201–233.

[13] R.A. Stephenson, The equilibrium field near the tip of a crack for finite plane strain deformations of incompressible elastic materials, J. Elasticity 12 (1982) 65–99.

[14] K.Ch. Le, H. Stumpf, The singular elastostatic field due to a crack in rubberlike materials, J. Elasticity 32 (1993) 183–222.

[15] P.H. Geubelle, W.G. Knauss, Finite strains at the tip of a crack in a sheet of hyperelastic material: I. Homogeneous case, J. Elasticity 35 (1994) 61–98.

[16] J.H. Chang, E.B. Becker, Finite element calculation of energy release rate for 2-d rubbery material problems with non-conservative crack surface tractions, Int. J. Num. Meth. Eng. 33 (1992) 907–927.